Engineering and Technology Journal
Journal homepage: https://etj.uotechnology.edu.iq

High Gain Transformer-less Inverter Based-on Capacitor Clamping Multi-phase Boost Converter

Oday S. Fares*, **Jasim F. Hussein**

Electrical Engineering Dept., University of Technology-Iraq, Alsina'a Street, 10066 Baghdad, Iraq.
*Corresponding author Email: eee.19.20@grad.uotechnology.edu.iq

HIGHLIGHTS

- High gain Non-isolated DC/DC converter based on clamper circuit is presented.
- Interleave inductor technique for current and voltage ripple reduction, two clamper circuits for voltage gain enhancing.
- Mathematical and simulation gain is 15 at 93.4% efficiency, and switch stress is 33% of V_{out}.

ARTICLE INFO

Handling editor: Jawad K. Ali

Keywords:
DC converter
Voltage gain
Switches voltage stress
Clamper circuit, Voltage ripple.

ABSTRACT

The boosting converters integrated with inverters are widespread use in many applications under transformer fewer inverter titles, including powered vehicles, PV systems, fuel cells systems, etc. Reliability, quality, maintainability, and reduction in size are important requirements in the energy conversion process. The multi-phase boost converter can be a good solution for high-power applications. The multi-phase boost enhanced by clamping capacitor structure provides low ripple, high gain, and evident improvement in the efficiency compared to the conventional converters. This paper investigates the transformer less inverter based on a capacitor clamping multi-phase boost converter. High gain proposed architectures are being designed to step-up voltage. The converter features a high voltage gain and offers additional solutions based on the capacitor clamping structure. The proposed architectures are being designed to optimize the gaining in popularity as they are increasing the voltage gain and the efficiency and mitigating the switching frequency effect. The investigation of validation performance was introduced through the steady-state analysis and operation. The operation modes and mathematical analysis are presented. To validate the performance in terms of input and output ripple and values, the converters were tested using MATLAB / SIMULINK. The results supported the mathematical analysis. The voltage gains increase reduces ripple in input current, and the output voltage is significantly detected. The switches stresses at the converter side are One-third of the output voltage.

1. Introduction

As the need for electricity grows, renewable energy sources are becoming more important (photovoltaic cells, fuel cells, UPS, and others). It has become important because of its carbon-reducing properties. They help minimize greenhouse gas emissions. To reduce reliance on fossil fuels, renewable energy has become very important as an environmentally friendly source. When sunlight strikes PV, DC electricity is generated, but it is of low unregulated voltage and high current [1,2]. As a result, a device to increase and regulate the voltage of renewable energy sources plays an essential role. Therefore, using a dc boost converter is more important to raise the value of output DC voltage to be suitable for the DC-grid or AC distribution system [3]. There are two types of DC converters, isolated and non-Isolated DC-DC converters.

In an isolated DC-DC boost converter, the main idea is to use a transformer to increase the transformation ratio by controlling the transformer turns ratio. However, using a transformer has the disadvantage of increasing converter size and cost and copper losses due to increased leakage inductance on the high voltage side. In addition, there are increases in switching losses. Therefore, the main disadvantage of the isolated converter is the transformer that increases the converter's losses, size, and cost. Therefore, the use of a non-isolated converter will solve this problem. The fundamental advantage of a non-isolated converter is that it is an excellent choice for low-power applications that need the use of renewable energy sources. Besides the small size, low cost, lower conduction losses, and higher efficiency [3,4].

http://doi.org/10.30684/etj.2022.131337.1028
Received 1 September 2021; Accepted 10 April 2021; Available online 20 June 2022
2412-0758/University of Technology-Iraq, Baghdad, Iraq

Theoretically, the output voltage in the conventional non-isolated boost converter depends on the switching time state (ON-OFF) conditions ($V_O = \frac{V_{IN}}{1-D}$) . Where $D = \frac{T_{on}}{(T_{on}+T_{off})}$. Because of component resistance, the increase of the duty cycle is limited (0.8). Therefore the voltage gain is limited in the conventional converter. Another conventional converter disadvantage of high input current ripple caused a lifetime reduction for renewable energy sources, High conduction losses, and high voltage stress across switch and power diode. ($V_{stress} = V_O$) [5-7]. At the same time, increasing the current stress passing throw the power device ($I_{stress} = I_{in}$). Therefore, a large filter component needs to reduce the ripple in output voltage and input current [6-8].

To overcome the conventional boost converter drawback, the proposed converter suggested combining two structures to improve the conventional boost converter features. The first structure is used of (N) number of parallel inductors. This structure decreases the ripple in the input current due to multi-phase inductors where current is distributed across them, simultaneously decreasing the conduction losses. Therefore there are improvements in efficiency and faster transient response. Besides that, the voltage ripple in the output voltage is reduced, but the voltage gains and voltage and current stress are the same as in a conventional boost converter [8-12].

The second structure is used two parallel clamper capacitors that produce an extra gain in output voltage, decreasing voltage stress on the power device and reducing the conduction losses. Therefore, the efficiency has improved [12-17].

This paper introduces the proposed converter with the following advantages:

- Increase voltage gain
- Reduce output voltage ripple
- Reduce input current ripple
- Reduce the voltage and current stress
- Reduce the conduction losses
- Improve the converter efficiency

The proposed converter can be utilized with a transformer-less inverter application since the converter voltage is suitable for converting to AC voltage without needing to use a transformer. Besides that, the transformer disadvantage of the increasing system size, cost, and copper losses lead to system efficiency reduction [17].

2. Transformer-Less Inverter Based-on Capacitor Clamping Multi-Phase Boost Converter Analysis

The proposed converter is shown in Figure 1. It is constituted of a two-structure dc converter and transformer-less inverter. The dc converter is made up of two structures. The first structure comprises three channels containing an inductor and switch connected in a parallel arrangement. The second structure of the dc converter is a capacitor clamping structure made of four diodes and three capacitors. The transformer-less inverter comprises switches and filter circuits of inductor and capacitor.

2.1 Capacitor Clamping Multi-Phase Boost Converter Analysis

The proposed converter is shown in Figure 1, and it consists of three shared inductors and switches controlled by three operation signals with a 120-degree phase shift between the first and second signal and between the second and third signal. The proposed converter operation signal waveform is shown in Figure 2.

There are six modes of operation for a proposed converter. The converter at continuous conduction mode operation during the steady-state through one period is discussed respectively as follows:

2.1.1 Mode I

As shown in Figure 3, the three switches (S_1, S_2 and S_3) are turned ON. Thus, the diodes D_1, D_2, D_3 and D_4 tended to turn OFF (reverse bias state). This action is led to causes storage energy in L_1, L_2, L_3. C_{out} are discharged its energy towards the inverter side, while C_{out} discharged its energy to R_L.

$$V_{in} = L_3 \frac{di_{L3}}{dt} = L_2 \frac{di_{L2}}{dt} = L_1 \frac{di_{L1}}{dt} \quad (1)$$

$$V_{c3} = V_{IN\ inverter} \quad (2)$$

$$V_{c\,out} = V_{out} = I_{out} R_L \quad (3)$$

2.1.2 Mode II

As shown in Figure 4, S_1, S_3 keep ON while S_2 is turned OFF. So, the diodes D_1, D_3 and D_4 are reverse bias states. Whereas D_2 is in ON state (forward-biased).In the second mode, the inductors L_1 and L_3 are stored energy with a positive slope of $\frac{V_{in}}{L}$ where $L = L_1 = L_2 = L_3$. At the same time, the supply of energy V_{in} and the stored energy in L_2 are transfer energy in series to C_1 .Furthermore, C_3 discharged its energy as inverter input voltage while C_{out} discharged its energy to R_L.

$$V_{in} = L_3 \frac{di_{L3}}{dt} = L_1 \frac{di_{L1}}{dt} \quad (4)$$

$$V_{in} - L_2 \frac{di_{L2}}{dt} - V_{c1} = 0 \quad (5)$$

$$V_{c3} = V_{IN\ inverter} \quad (6)$$

$$V_{c\ out} = V_{out} = I_{out}R_L \quad (7)$$

2.1.3. Mode III

(S_1, S_2 and S_3) are ON state. So is equivalent to mode I.

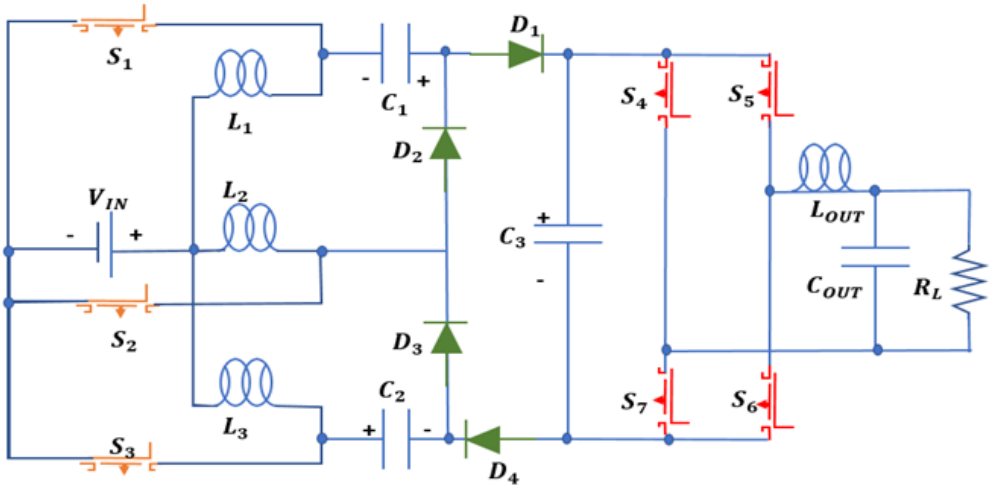

Figure 1: Proposed converter circuit diagram

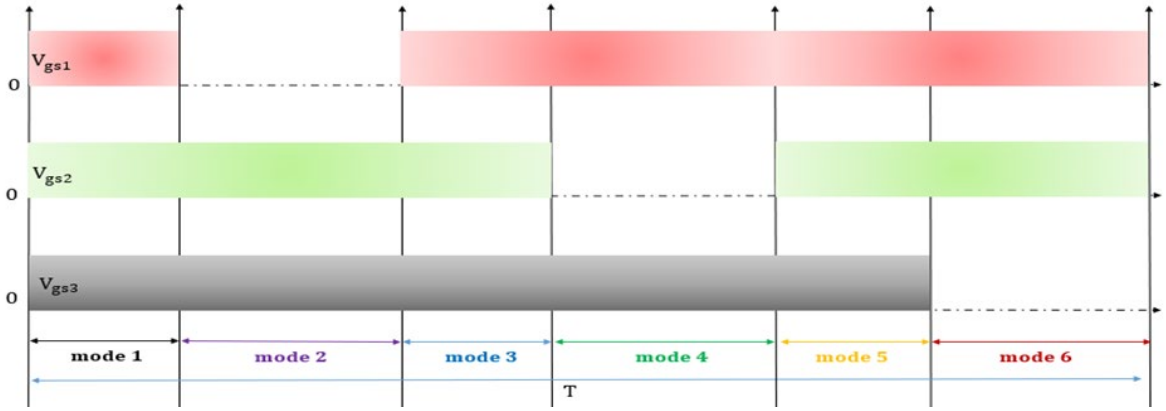

Figure 2: Modes of operation for the proposed converter

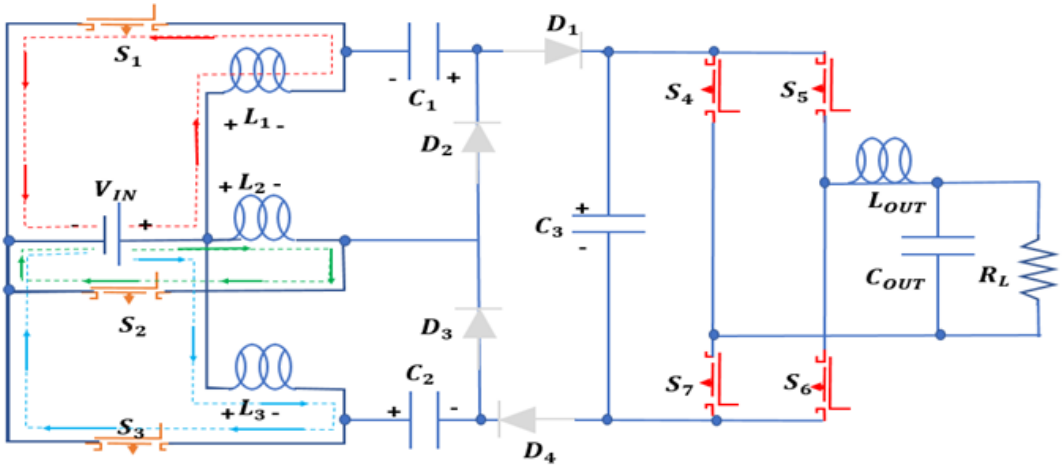

Figure 3: Mode 1, Mode 3, and Mode 5 of the proposed converter operation

2.1.4. Mode IV:

As shown in Figure 5, S_3 is turned off while $S_1$and S_2 kept tured on. So, the diodesD_1, $D_2$and D_4 are reverse bias states. Whereas $D_3$is in ON state (forward-biased).In the fourth mode, the inductors $L_1$and L_2 are stored energy with a positive slope

of $\frac{V_{in}}{L}$ where $L = L_1 = L_2 = L_3$. At the same time, the supply of energy V_{in} and the stored energy in L_3 are transfer energy in series to C_2. Furthermore, C_3 discharged its energy as inverter input voltage and C_{out} discharged its energy to R_L.

$$V_{in} = L_2 \frac{di_{L2}}{dt} = L_1 \frac{di_{L1}}{dt} \quad (8)$$

$$V_{in} - L_3 \frac{di_{L3}}{dt} - V_{C2} = 0 \quad (9)$$

$$V_{c3} = V_{IN\ inverter} \quad (10)$$

$$V_{c\,out} = V_{out} = I_{out} R_L \quad (11)$$

2.1.5. Mode V:

S1, S2, and S3 all are on. The operating principle is the same as mode I

2.1.6. Mode VI:

As shown in Figure 6, S_1 is turned off while $S_2$and S_3 keep turning-on. So, the diodes$D_2$and D_3 are reverse bias states. Whereas $D_1$and $D_4$is in ON state (forward-biased).In the sixth mode, the inductors $L_2$and L_3 are stored energy with a positive slope of $\frac{V_{in}}{L}$ where $L = L_1 = L_2 = L_3$. At the same time, the supply of energy V_{in} and the stored energy in L_1 are transfer energy in series with V_{c1} and V_{C2} transfer energy to C_3 At the same time C_3 discharged its energy as inverter input voltage while C_{out} discharged its energy to R_L.

$$V_{in} = L_2 \frac{di_{L2}}{dt} = L_3 \frac{di_{L3}}{dt} \quad (12)$$

$$V_{in} - L_1 \frac{di_{L1}}{dt} - V_{C1} - V_{C2} + V_{Cout} = 0 \quad (13)$$

$$V_{c3} = V_{IN\ inverter} \quad (14)$$

$$V_{c\,out} = V_{out} = I_{out} \quad (15)$$

2.2 Inverter Analysis

The analysis of an inverter uses the sinusoidal bipolar pulse width modulation technique to control the operation of switches, as shown in Figure 7. There are two modes of operation.

2.2.1. Mode 1:

In this mode, S_5 and S_7 are ON while S_4 and S_6 are OFF, as shown in Figure 8-a. This mode is done when the voltage value of the reference signal is larger than the voltage of the carrier signal.

$$V_{sine} > V_{tri} \rightarrow V_{out} = +V_{in} \quad (16)$$

2.2.2. Mode 2:

In this mode $S_4$and S_6 are ON $S_5$and S_7 are OFF, as shown in Figure 8-b. This mode is done when the voltage value of the reference signal is larger than the voltage of the carrier signal.

$$V_{sine} < V_{tri} \rightarrow V_{out} = -V_{in} \quad (17)$$

2.3 Proposed Converter Steady-State Analysis.

2.3.1. Voltage gain:

According to the volt-second balance principle on L_1, L_2, L_3., can be obtained: According to the volt-second balance principle on inductor L_2 the output capacitor voltage is shown in Figure 9.

$$\left.\begin{cases} V_{Lavg} = V_{in} * t_{on} + (V_{in} - V_{c3} + V_{c1} + V_{c2}) * t_{off} = 0 \\ \quad where \qquad t_{on} = D \quad , \quad t_{off} = (1 - D) \\ V_{Lavg} = DV_{in} + (1 - D)(V_{in} - V_{c3} + V_{c1} + V_{c2}) = 0 \\ V_{c3} = (V_{in}/(1 - D)) + (V_{c1} + V_{c2}) \end{cases}\right\} \quad (18)$$

Also, according to the volt-second balance principle on the inductor L_2 the capacitor 1 voltage is shown in Figure 9.

$$V_{in} - V_{c1}(1 - D) = 0 \quad so \quad V_{c1} = \frac{V_{in}}{1-D} \quad (19)$$

At last, according to the volt-second balance principle on the inductor L_3 the capacitor 2 voltage is shown in Figure 9.

$$V_{in} - V_{c2}(1-D) = 0 \quad so \quad V_{c2} = \frac{V_{in}}{1-\mathrm{D}} \tag{20}$$

By subtiuting equations 19 and 20 in 18, we get:

$$V_{c3} = V_{IN\ inverter} = \frac{V_{in}}{1-\mathrm{D}} + (V_{c1} + V_{c2}) = \frac{V_{in}}{1-\mathrm{D}} + \frac{V_{in}}{1-\mathrm{D}} + \frac{V_{in}}{1-\mathrm{D}} = 3\frac{V_{in}}{1-\mathrm{D}} \tag{21}$$

$$\mathrm{M} = \frac{\mathrm{V}_{c3}}{V_{in}} = \frac{3}{1-\mathrm{D}} \quad where\ \mathrm{M}= \text{dc converter voltage gain} \tag{22}$$

The average output voltage from the inverter is dependent on $\boldsymbol{m_a}$, where $\boldsymbol{m_a}$(modulation index) and its change sinusoidally with variable duty cycle.

$$\mathrm{m_a} = \left(\frac{V_{ref}}{V_{tri}}\right) \tag{23}$$

$$V_{o,avg} = \mathrm{m_a} V_{dc} \tag{24}$$

$$V_{o,avg} = V_{dc} * \left(\frac{V_{ref}(t)}{V_{tri}}\right) \tag{25}$$

$$V_{o,avg} = V_{dc} * (V_{p,ref} sin\omega t / V_{tri}) \tag{26}$$

$$V_{o,avg} = V_{dc} * \mathrm{m_a}\ sin\omega t \tag{27}$$

$$V_{o,avg} = V_{c3} * \mathrm{m_a}\ sin\omega t \tag{28}$$

2.3.2. The proposed dc converter Output voltage ripple

In the proposed dc converter, the ripple of the output voltage can be reduced because the output voltage frequency is three times more than the switching frequency, as shown in Figure 9.

$$\mathrm{V_{ripple}} = \frac{\Delta \mathrm{V_o}}{\mathrm{V_o}} = \frac{\mathrm{D}}{3\mathrm{F}_{sw}\mathrm{CR_L}} \tag{29}$$

2.3.3. Semiconductor voltage stress

2.3.1.1 Voltage stress across the switches:

From mode 2, the voltage stress across the switch S_2 when the switch is in an off state, hence.

$$\mathrm{V_{S2\ stress}} = \frac{\mathrm{V_{in}}}{1-\mathrm{D}} = \frac{V_o}{3} \tag{30}$$

And from mode 4, the voltage stress across the switch S_3 when the switch is in an off state, hence.

$$\mathrm{V_{S3\ stress}} = \frac{\mathrm{V_{in}}}{1-\mathrm{D}} = \frac{V_o}{3} \tag{31}$$

In the same way and from mode 6, the voltage stress across the switch S_1 when the switch is in an off state:

$$\mathrm{V_{S1\ stress}} = \frac{\mathrm{V_{in}}}{1-\mathrm{D}} = \frac{V_o}{3} \tag{32}$$

The voltage stress across switches concerning modes of operation is shown in Figure

2.3.1.2 Voltage stress across the diodes:

When a diode is reverse biased, the voltage stress across it is as follows:
Voltage stress across D_1 pass in two stages:
stage 1(mode 2) and Stage 2 (mode 4) when diode in reverse biasing. Therefore, the diode is an open circuit.

$$\mathrm{V_{D1\ stress}} = \mathrm{V_{Cout}} - (\mathrm{V_{C1}} + \mathrm{V_{C2}}) = \frac{\mathrm{V_{in}}}{1-\mathrm{D}} = \frac{\mathrm{V_{out}}}{3} \tag{33}$$

$$\mathrm{V_{D1\ stress}} = \mathrm{V_{Cout}} - \mathrm{V_{C1}} = \mathrm{V_{D1\ stress}} = \frac{2\mathrm{V_{in}}}{1-\mathrm{D}} = \frac{2\mathrm{V_{out}}}{3} \tag{34}$$

Voltage stress across D_2 pass in two stages: stage 1 (mode 4) and Stage 2 (mode 6) when the diode is in reverse biasing. Therefore, the diode is an open circuit.

$$V_{D2\ stress} = V_{C1} = \frac{V_{in}}{1-D} = \frac{V_{out}}{3} \quad (35)$$

$$V_{D2\ stress} = V_{Cout} - V_{C2} = \frac{2V_{in}}{1-D} = \frac{2V_{out}}{3} \quad (36)$$

Voltage stress across D_3 pass in two stages:
Stage 1(mode 2) and Stage 2 (mode 6) when diode in reverse biasing, Therefore, the diode as an open circuit.

$$V_{D3\ stress} = V_{C2} + V_{C1} = \frac{2V_{in}}{1-D} = \frac{2V_{out}}{3} \quad (37)$$

$$V_{D3\ stress} = V_{C2} = \frac{V_{in}}{1-D} = \frac{V_{out}}{3} \quad (38)$$

The voltage stress across diodes concerning modes of operation is shown in Figure 10.

3. Simulation

The parameter of the proposed DC-DC converter is listed in Table 1. The MATLAB R2018B is used to simulate the converter. The three DC converter control signals have a difference in phase shift of 120 degrees, as in Figure 11. The switches voltage stress is 125V as in Figure 12, input voltage = 24V, output converter voltage = 360V and output inverter voltage = 310V as in Figure 13, the capacitor voltage of $C_1, C_2 C_3, and\ C_{out}$ are shown in Figure 14. The diodes voltage stress =250 V, as in Figure 15. The voltage waveform of the three inductors is shown in Figure 16. The MATLAB simulation schematic of transformer-less inverter based-on capacitor clamping multi-phase boost converter is shown in Figure 17.

From the simulation results, it appears that it validates the mathematical calculation where the output voltage is equal to $V_{out} = V_{IN\ inverter} = 3\frac{V_{in}}{1-D} = 360$ Volt, the voltage stress across switches is equal to $\frac{V_{in}}{1-D} = 120$ Volt, and the stress across diodes is equal to $\frac{2V_{in}}{1-D} = 240$ Volt in two diodes and 120 Volta in the other two diodes.

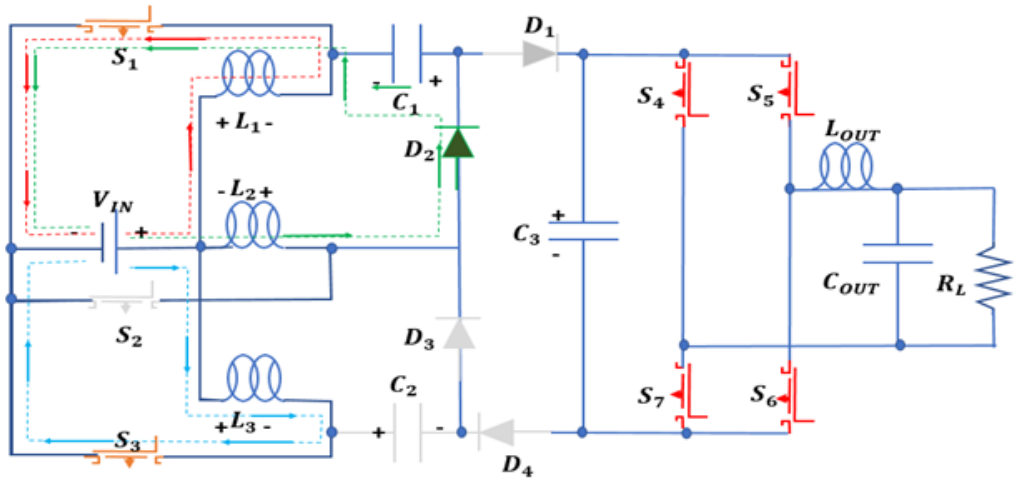

Figure 4: Mode 2 of the proposed converter operation

Table 1: Parameter of the proposed converter

Parameter	value
L_1, L_2, L_3	800 µH
C_1, C_2, C_3	25 µF
The duty cycle of switches S_1,S_2 and S_3 (D)	0.8
Switching Frequency - f_{sw}	25 kHz
Input Voltage	24 V
Dc converter Output Voltage	360 V

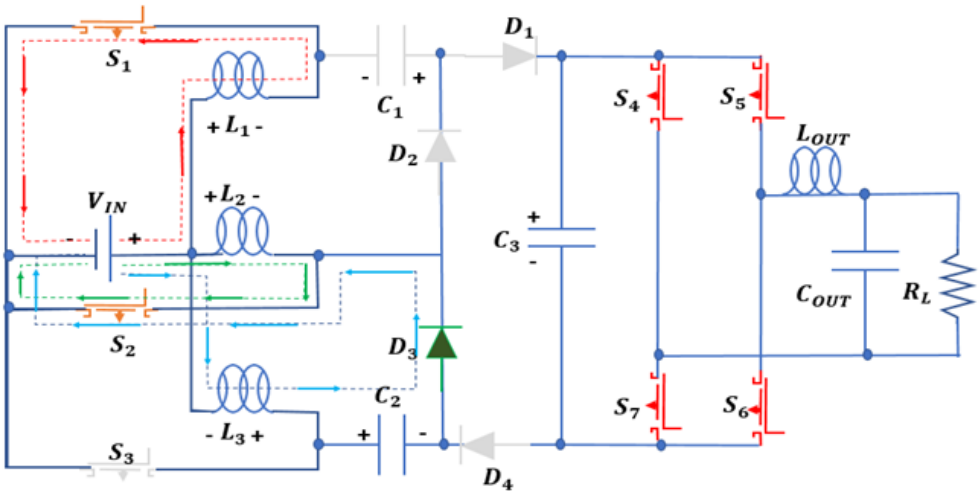

Figure 5: Mode 4 of the proposed converter operation

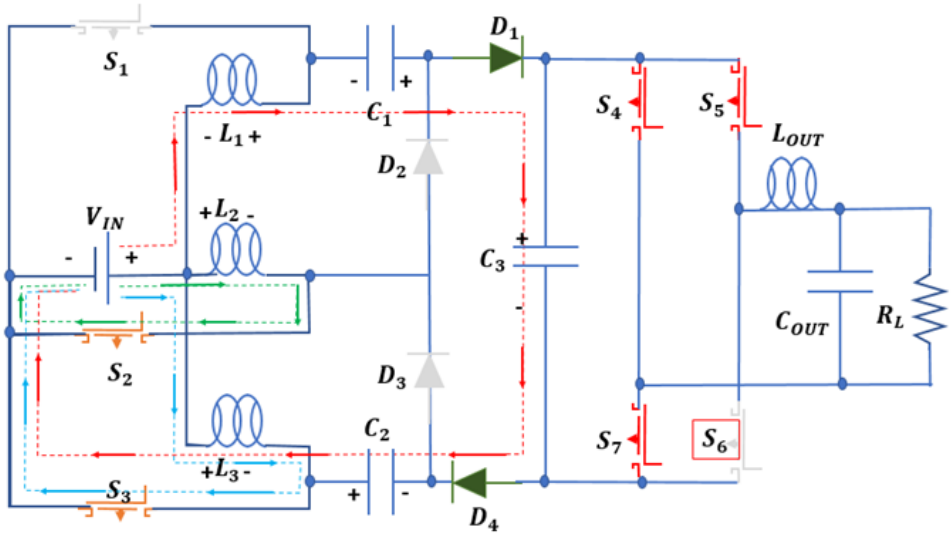

Figure 6: Mode 6 of the proposed converter operation

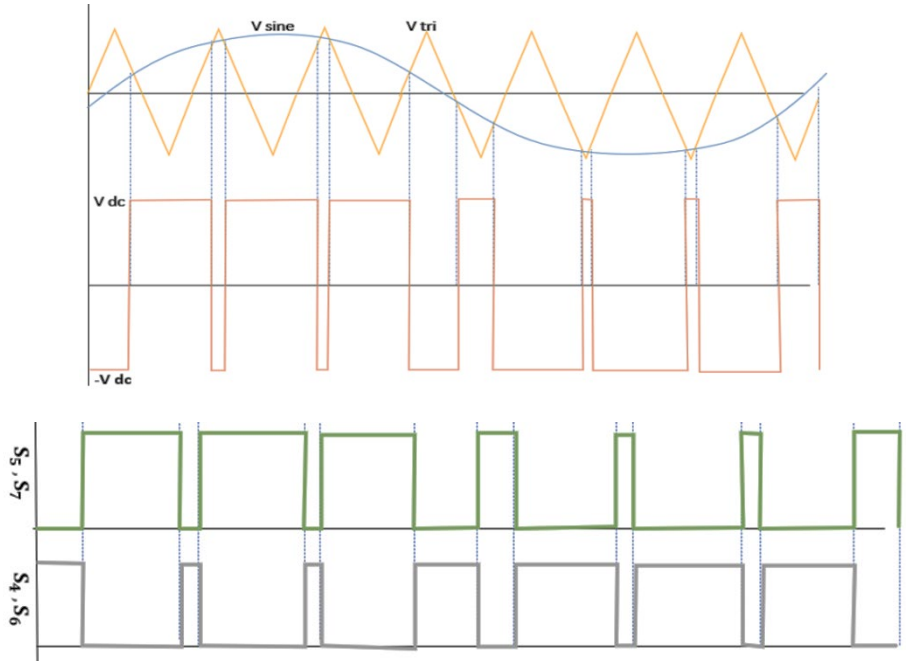

Figure 7: Sinusoidal bipolar pulse width modulation technique operation waveform

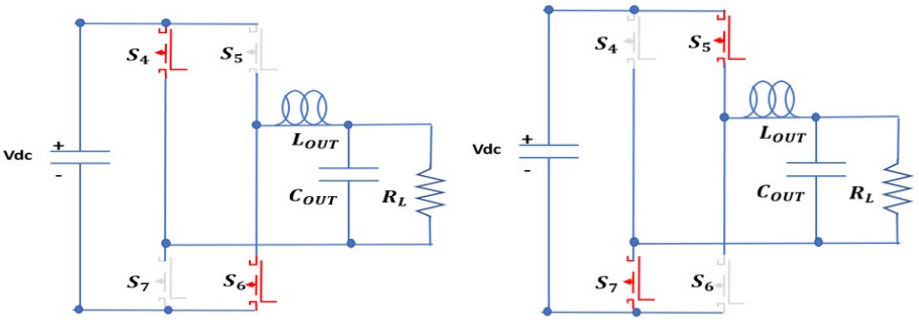

Figure 8: a. Mode 1 b. Mode 2

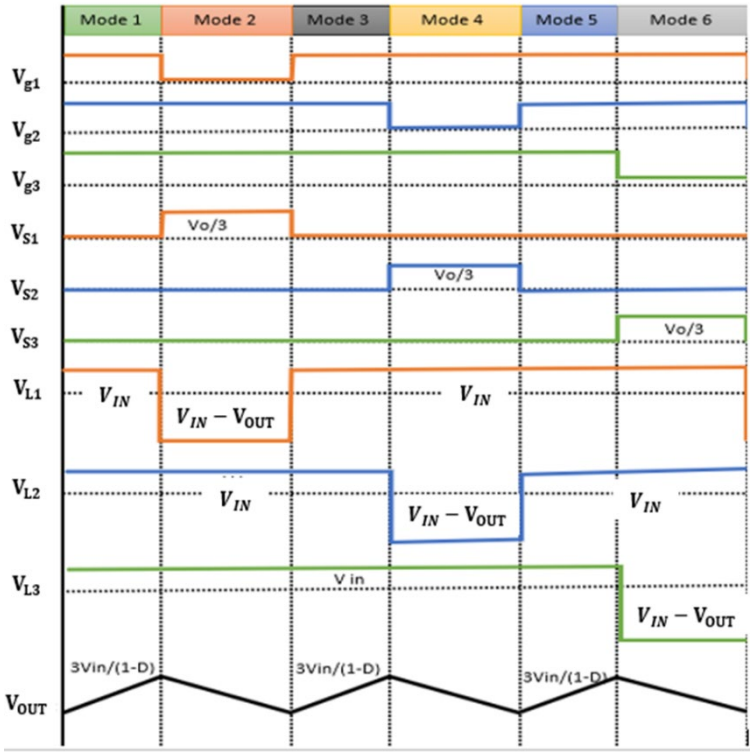

Figure 9: key waveform for the proposed dc converter

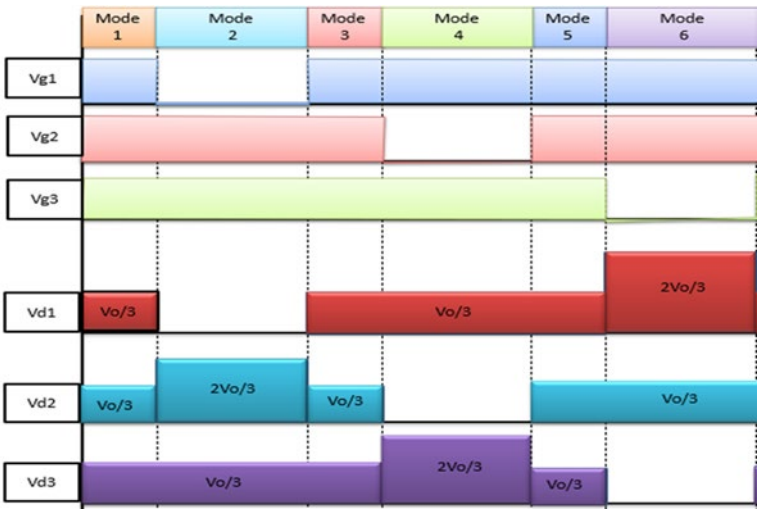

Figure 10: Voltage stress across switches waveform

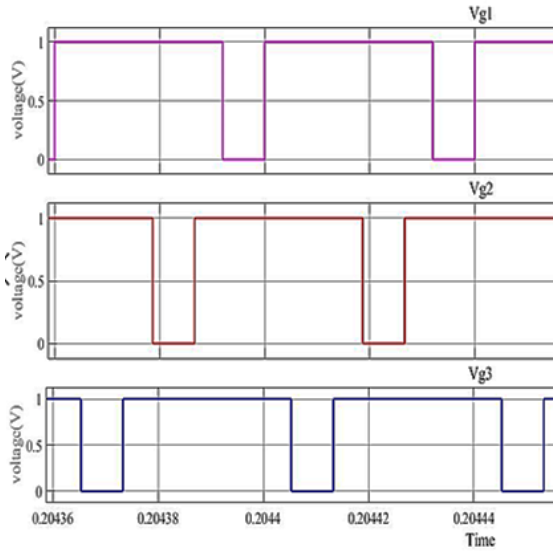

Figure 11: Voltage switch waveform control

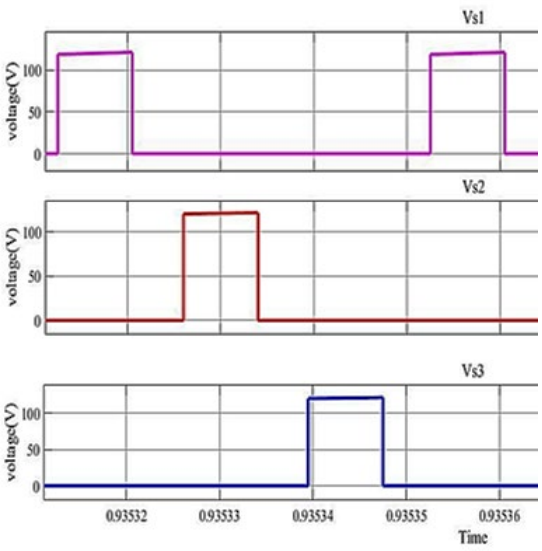

Figure 12: Switches voltage stress waveform

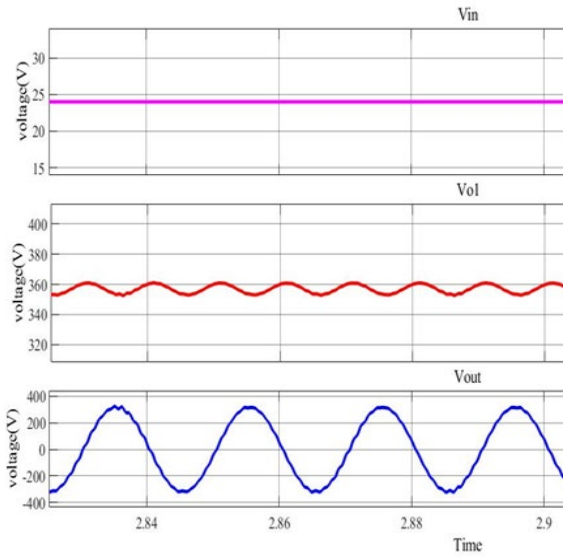

Figure 13: Converter and inverter Output voltage

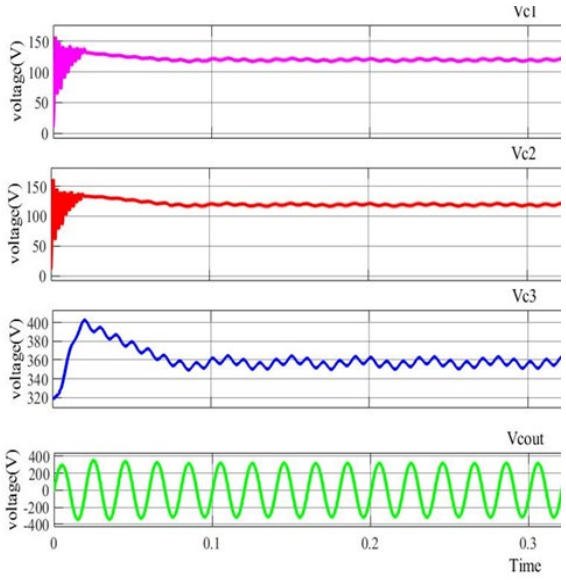

Figure 14: Capacitors voltage waveform

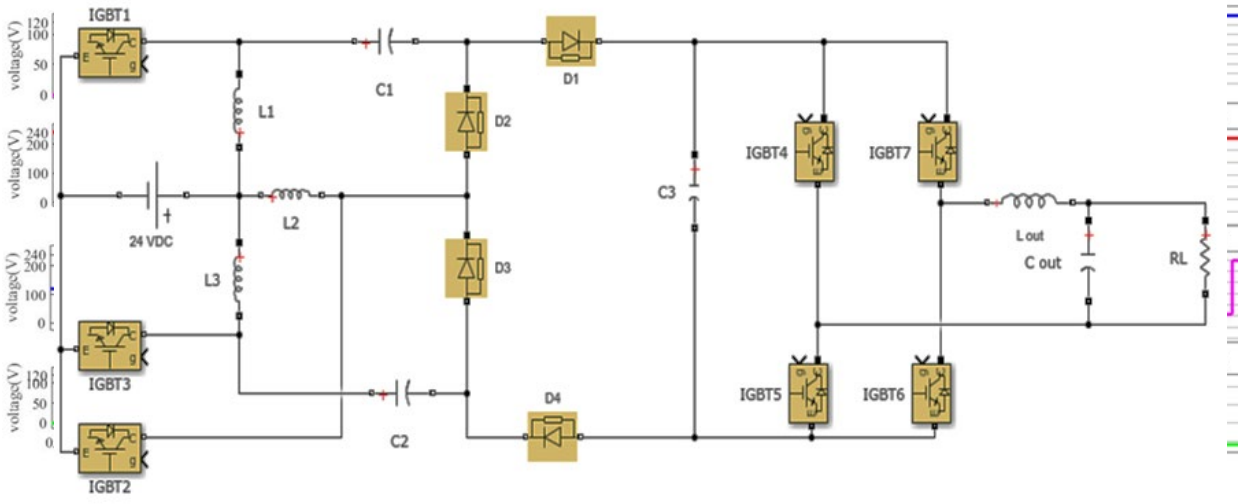

Figure 17: Schematic of transformer-less inverter based-on capacitor clamping multi-phase converter

4. Conclusion

The non-isolated DC-DC boost converter proposed in this study comprises two constructions (three shared inductors and a clamper capacitor circuit). This converter is fed by a single source of input. The converter has a high transformation ratio and lower voltage stress across power devices (switches and diodes).and the second circuit is the transformer-less inverter. The suggested converter is ideal for power applications using renewable energy sources (photovoltaic, fuel cell, and UPS). This is because the source's input current will be continuous and have the least ripple. The analysis of the proposed converter and its design was demonstrated in this work, and it was verified using MATLAB Simulation. The efficiency of the suggested converter is 93.5 percent due to the transformer-less inverter. In addition, the total cost of the converter will be decreased due to lower voltage stress across the power device and the lack of a transformer.

Acknowledgment

I cannot express enough thanks to the supervising doctor for his continuous support and encouragement: Dr. Jasim Farhoud Hussain. I offer my sincere appreciation for the learning opportunities he has provided me.

This scientific paper could not have been completed without his continuous support and guidance to me, either directly within the university through repeated meetings or indirectly through social media. My sincere thanks.

Author contribution

All authors contributed equally to this work.

Funding

This research received no specific grant from any funding agency in the public, commercial, or not-for-profit sectors.

Data availability statement

The data that support the findings of this study are available on request from the corresponding author.

Conflicts of interest

The authors declare that there is no conflict of interest.

References

[1] L. A. Soriano, P. Ponce, A. Molina, Analysis of DC-DC Converters for Photovoltaic Applications based on conventional MPPT Algorithms, Int.Conf. Electr. Eng. Comput. Sci. Aut. Control, (2017) 1-6. https://doi.org/10.1109/ICEEE.2017.8108884

[2] T. Xue, Z. Minxin ,Y. Songtao, Maximum power point tracking for photovoltaic power based on the improved interleaved boost converter, IEEE Conf. Ind. Electron. Appl., (2016) 2215-2218 .http://dx.doi.org/10.1109/ICIEA.2016.7603957

[3] G. Ganesan, M. Prabhakar, A novel interleaved boost converter with voltage multiplier cell, IEEE Int. Conf. Electr .Energy Systد. (ICEES), Chennai, India, 2014, 183-188,. https://doi.org/10.1109/ICEES.2014.6924165

[4] A. Mittle, R. K. Singh, S. J. Chandra, A New Interleaved High Step-up DC-DC Converter, IEEE Stud. Conf .Eng. Syst . , (2019) 1-5. https://doi.org/10.1109/SCES46477.2019.8977225

[5] M. A. Salvador, T. B. Lazzarin, R. F. Coelho, High Step-Up DC-DC Converter with Active Switched-Inductor and Passive Switched-Capacitor Networks, IEEE Trans. Ind. Electron., 65 (2018) 5644-5654.https://doi.org/10.1109/TIE.2017.2782239

[6] S. Saravanan, N. R. Babu, A modified high step-up non-isolated DC-DC converter for PV application, J. Appl. Res. Technol., 15 (2017) 242–249. https://doi.org/10.1016/j.jart.2016.12.008

[7] A.Farooq, Z. Malik, D. Qu, A Three-Phase Interleaved Floating Output Boost Converter, Hindawi Publishing Corporation, Adv. Mater. Sci. Eng., 2015 (2015) 8. https://doi.org/10.1155/2015/409674

[8] M. L. Alghaythi, R. M. O'Connell, N. E. Islam , J. M. Guerrero, A Multiphase-Interleaved High Step-up DC-DC Boost Converter with Voltage Multiplier and Reduced Voltage Stress on Semiconductors for Renewable Energy Systems, IEEE PES Innov. Smart Grid Technol. Conf ., (2020) 1-5. https://doi.org/10.1109/ISGT45199.2020.9087696

[9] O. S. Fares, J. F. Hussein, High gain multi-phase boost converter based-on capacitor clamping structure, J. Electr. Eng. Comput. Sci., 24 (2021) 689-696. http://doi.org/10.11591/ijeecs.v24.i2.pp689-696

[10] S. K. Waghmare, A. Deshpande, Performance Analysis and Comparison of Conventional and Interleaved DC/DC Boost Converter Using MULTI SIM, IJAREEIE., 4 (2015) 2297- 2303.

[11] K. S. Faraj, J. F. Hussein, Analysis and Comparison of DC-DC Boost Converter and Interleaved DC-DC Boost Converter, Eng. Technol. J., 38 (2020) 622-635. https://doi.org/10.30684/etj.v38i5A.291

[12] M. E. Azizkandi, F. Sedaghati, H. Shayeghi, A New Boost DC-DC Converter Based on a Coupled Inductor and Voltage Multiplier Cells, Int. j. ind. electron. control. optim., 2 (2019) 265-278. https://doi.org/10.22111/IECO.2019.28215.1127

[13] A. Alzahrani, P. Shamsi, M. Ferdowsi, A novel interleaved non-isolated high-gain DC-DC boost converter with Greinacher voltage multiplier cells, 2017 IEEE 6th International Conference on Renewable Energy Research and Applications (ICRERA), San Diego, CA, USA, 2017, 222-227 https://doi.org/10.1109/ICRERA.2017.8191270

[14] H. Li, W. Wang, Y. Zeng, Y. Zhao, A 3L Capacitor Clamping DC-DC Converter with Low Current Ripple and High Voltage Gain, in: IEEE Energy Conversion Congress and Exposition., 29 (2019) 3. https://doi.org/10.1109/ECCE.2019.8912843

[15] B. Sri Revathia, P. Mahalingama, F. G. Longattb , Interleaved high gain DC-DC converter for integrating solar PV source to DC bus, Sol. Energy, 188 (2019) 924-934. https://doi.10.1016/j.solener.2019.06.072

[16] N. Tewari, V.T. Sreedevi, A novel single switch dc-dc converter with high voltage gain capability for solar PV based power generation systems, Solar Energy, 171 (2018) 466-477. https://doi.org/10.1016/j.solener.2018.06.081

[17] F. F. Salih, O. A. Ahmed, Improved Y-Source Single-Stage Transformer less Microinverter for PV Residential Applications, Eng. Technol. J., 38 (2020) 1327-1341.https://doi.org/10.30684/etj.v38i9A.1143.